The austenite grain structure of low-alloy steel weld deposits

H. K. D. H. BHADESHIA
Department of Metallurgy and Materials Science, Univeristy of Cambridge, Cambridge, UK

L.-E. SVENSSON, B. GRETOFT
ESAB AB, Gothenburg, Sweden

The shape of austenite grains in low-alloy steel submerged-arc weld deposits has been examined; it is found that the grain morphology can be approximated as a honeycomb of hexagonal prisms with their "c" axes aligned along the major heat-flow direction. Methods of determining the grain size from simple stereological measurements are also discussed. An increase in the oxygen content has not been found to reduce the austenite grain size of as-deposited welds.

1. Introduction

Solidification in low-alloy steel weld deposits involves the epitaxial growth of delta-ferrite (δ) from parent-plate grains at the fusion boundary [1–3], and because of the high temperature gradients involved in arc-welding, it proceeds in a cellular manner [4]. The resulting δ-ferrite grains have an anisotropic columnar morphology, with their major axes following the direction of maximum heat flow. On further cooling, austenite (γ) allotriomorphs nucleate at the δ/δ cell-boundaries and anisotropic γ growth along these boundaries leads to the formation of columnar γ grains which closely resemble the original δ-ferrite morphology. The γ grains can sometimes be finer than the δ grains if the nucleation rate at δ/δ grain boundaries is high [5]. If the cooling rate, carbon or the substitutional alloy content is sufficiently high, then γ is the first solid to form and columnar γ grains (nucleated epitaxially at the fusion boundary) grow directly from the melt [6–8].

The γ grain structure has a major influence on the subsequent development of microstructure during cooling of the weld deposit. Recent work [9] has demonstrated quantitative relationships between the γ grain size and the volume fractions of allotriomorphic, Widmanstätten and acicular ferrite obtained in the final microstructure. The morphology of the columnar austenite grains was approximated as space-filling hexagonal prisms of cross-sectional side length "a" and height "c", where $c \gg a$ with the c axes all aligned normal to the temperature isotherms. This morphology is consistent with cellular solidification, in which the solid–liquid interface consists of a honeycomb structure [10]. One of the aims of this study is to establish whether the hexagonal prism shape is an adequate representation of the actual γ grain structure.

It has sometimes been suggested [11–14] that an increase in inclusion content should, due to boundary pinning, lead to a decrease in the γ grain size of weld

deposits. The volume fraction of inclusions in welds is known to directly correlate with the total oxygen content of the weld [12, 15] since most of the oxygen is present in the form of oxides. There is however, evidence [9] that the γ grain size is not influenced by variations in oxygen content within the range $267 \rightarrow 342$ p.p.m. (by weight). Our aim was also to investigate the role of inclusions in determining the γ grain size.

2. Experimental details

2.1. Weld preparation

The welds are deposited using the submerged-arc welding technique; the joint geometry is illustrated in Fig. 1. The submerged-arc method was chosen for its high deposition rate, which in turn leads to a large deposit size per run, so that stereological measurements using optical microscopy are easier to conduct. All measurements were carried out on the top layer which contained the as-deposited microstructure. The welding conditions and compositions of the wires and fluxes used are presented in Table I. The wire and flux combinations are specifically chosen to produce two welds (designated 1,2) with approximately identical carbon, manganese and silicon concentrations, but with different oxygen, titanium and sulphur concentrations since the latter elements correlate with the volume fraction of inclusions in the microstructure [12, 16]. Weld 1 therefore contains higher levels of oxygen and titanium but is otherwise similar to Weld 2 (Table I). The use of very high welding speeds (~ 17 mm sec^{-1}), especially in highly alloyed steels, can during solidification lead to a zone of equiaxed grains along the centre-line of the weld deposit [1, 16, 17], but these conditions are not valid for the present welds and no such zone was found on metallographic examination of transverse sections.

For equilibrium cooling, the low-carbon steels used in this investigation should solidify with δ-ferrite as the primary phase [6]. The work of Edvardson *et al.*
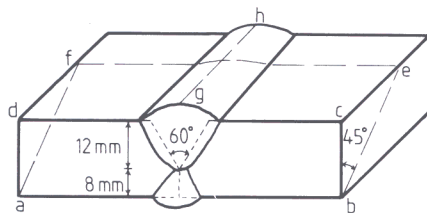
Figure 1 Diagram illustrating the joint geometry and the sections on which stereological measurements were carried out. The welding direction is along the line gh. The plane abcd represents the transverse section (i.e. normal to the welding direction), abef the inclined section and the longitudinal section contains the weld centre-line gh and is parallel to the plane bce.

[6] indicates that even with the rapid solidification rate associated with the welding process (maximum of 4.72 mm^{-1}, along the weld centre-line), δ-ferrite should still be the primary phase to form.

2.2. Quantitative metallography
Stereological measurements on welds are usually carried out on transverse sections; various empirical methods are then chosen to represent the nature of the

TABLE I Welding conditions and chemical compositions of the consumables used, and of the resulting weld deposits. The weld, wire and base plate compositions were determined spectroscopically, with the exception of oxygen and nitrogen, both of which were determined using Leco furnaces (Leco Ro-17 and Leco Tn-15), with 50 g of material for each determination to ensure representative results

Welding conditions (identical for both welds, with an interpass temperature of 100° C)

	Top layer
Voltage a.c. (V)	32
Current (A)	875
Welding speed (mm sec^{-1})	4.72
Nominal heat input (MJ m^{-1})	5.8

Flux compositions (wt %)

	Weld I	Weld 2
CaO + MgO	5	40
Al$_2$O$_3$ + MnO	50	15
SiO$_2$ + TiO$_2$	35	15
CaF$_2$	5	25

Wire and base plate compositions (wt %)

	Wire (Weld I)	Wire (Weld 2)	Base Plate
C	0.10	0.10	0.17
Si	0.25	0.02	0.41
Mn	1.00	0.50	1.32
Al	0.003	0.004	0.003
Ti	0.004	0.004	0.005
Nb	0.003	0.003	0.023
S	0.017	0.014	0.011

Deposit compositions (wt %, except oxygen and nitrogen in p.p.m. by weight)

	Weld I (top layer)	Weld 2 (top layer)
C	0.12	0.14
Si	0.49	0.33
Mn	1.16	1.22
Ti	0.020	0.005
Nb	0.018	0.013
Al	0.020	0.007
P	0.027	0.021
S	0.015	0.010
N	75	58
O	418	121

austenite grain structure. The γ grains appear elongated in transverse section and a measurement of the "width" in a direction normal to the major axis is usually taken to represent the "grain size". This procedure gives no information on the grain shape in three dimensions or the amount of grain boundary surface per unit volume. In this work our aim was to make statistically significant measurements of the shape of the grains and to examine the use of various stereological parameters as a way of representing the highly anisotropic grains that are found in welds. This is best achieved by examining the grain structure on different planes relative to the welding direction.

Consider a space-filling grain structure of uniformly sized hexagonal prisms with their c axes all aligned in the direction of columnar growth. The mean lineal intercept $\bar{L}$ and the mean areal intercept $\bar{A}$, obtained as an average of measurements from several differently oriented sections, are given [18] by

$$\bar{L} = 12^{0.5}ac/(3^{0.5}a + 2c) \qquad (1a)$$

for $c \gg a$, this becomes

$$\bar{L} = 3^{0.5}a \qquad (1b)$$

$$\bar{A} = 27^{0.5}a^2c/(3a + c) \qquad (2a)$$

for $c \gg a$, this becomes

$$\bar{A} = 27^{0.5}a^2 \qquad (2b)$$

The three different sections examined in the present work are transverse, longitudinal and 45° inclined sections, as illustrated in Fig. 1.

Lineal and areal intercept measurements were carried out on Quantimet 720 image analysing computer, using tracings of the γ grain structure from montages of micrographs taken at ×100 magnification. The low magnification is necessary in order to ensure sufficient numbers of complete sections of γ grains in the area examined. Edge errors were completely avoided by using a guard region which rejects information obtained from γ grains whose sections only partly lie within the area being analysed. For directional microstructures, the lineal intercept is a function of scan orientation relative to the microstructure, whereas Equation 1 requires that the test lines be randomly orientated with respect to the microstructure. Hence, each field was studied at 15 orientations of the scan direction, the orientations being set with the help of a random number generator.

3. Results and discussion
The anisotropic prior austenite grain structure, as revealed by the layers of grain boundary allotriomorphic ferrite is illustrated in Figs 2 and 3 for welds 1 and 2 respectively. Mean lineal and mean areal intercept measurements from the transverse, longitudinal and inclined sections (identified by the subscripts t, l and i respectively) are presented in Table II, where $\bar{L} = (\bar{L}_t + \bar{L}_l + \bar{L}_i)/3$ and $\bar{A} = (\bar{A}_t + \bar{A}_l + \bar{A}_i)/3$.

The errors in the measurements arise due to the finite number (N) of tests and due to the variability in the size of the features, as expressed by the standard deviation σ. Both of these effects can be taken into account by calculating the standard error (SE) of
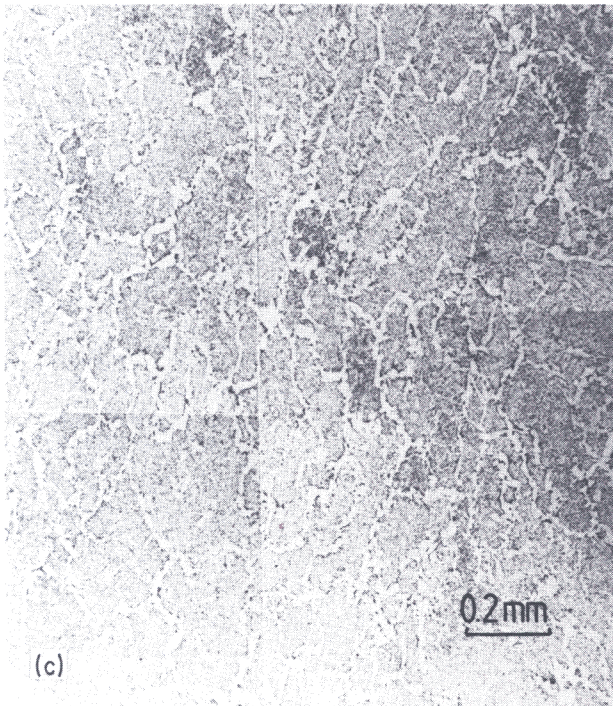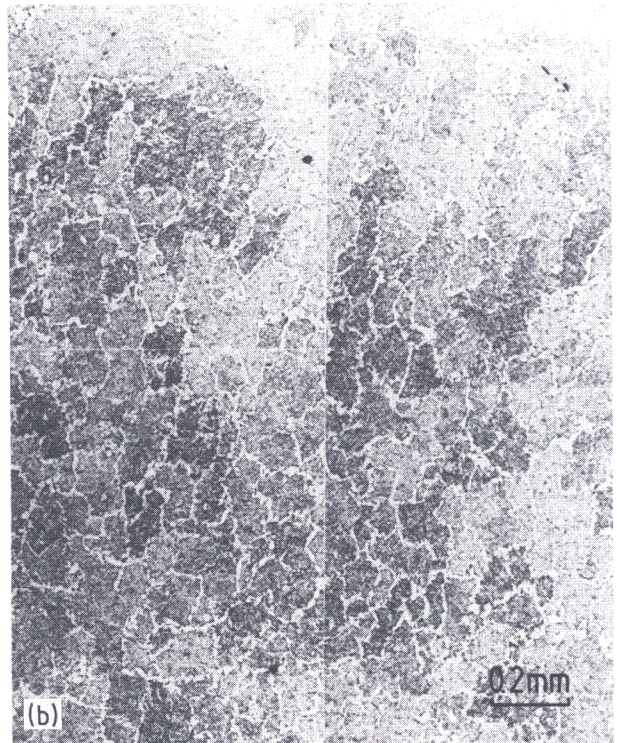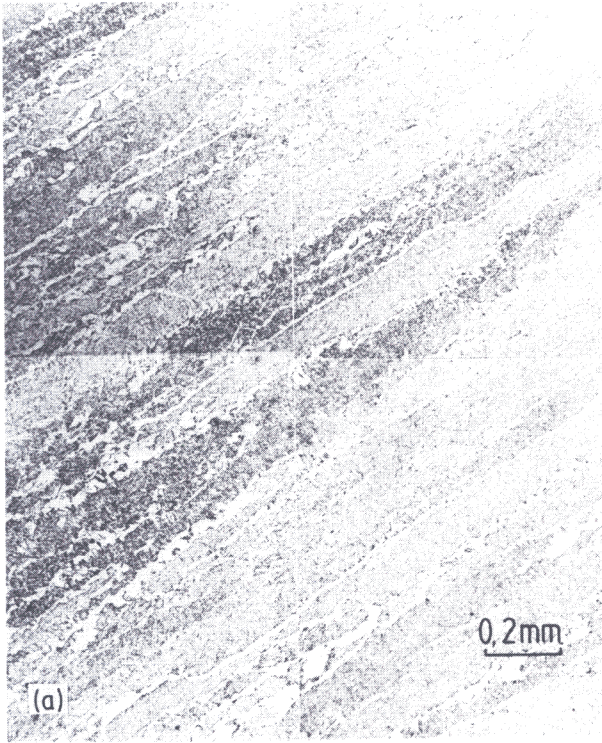
Figure 2 (a) Transverse, (b) longitudinal and (c) inclined sections from the top layer of Weld 1.

the mean [19], given by $SE = \sigma N^{-0.5}$. The standard errors for the areal intercept measurements are larger than those for the lineal intercept measurements primarily because of the difficulty in obtaining sufficient complete sections of the very large γ grains within the analysis frame.

As pointed out earlier, Equations 1 and 2 refer to averages of measurements from several differently orientated sections. The results can however be subjected to a more detailed analysis by expressing the intercept measurements as a function of the orientation of the plane of section. For the longitudinal sections, Figs 2 and 3 show an approximately equiaxed grain structure which may be regarded as the structure
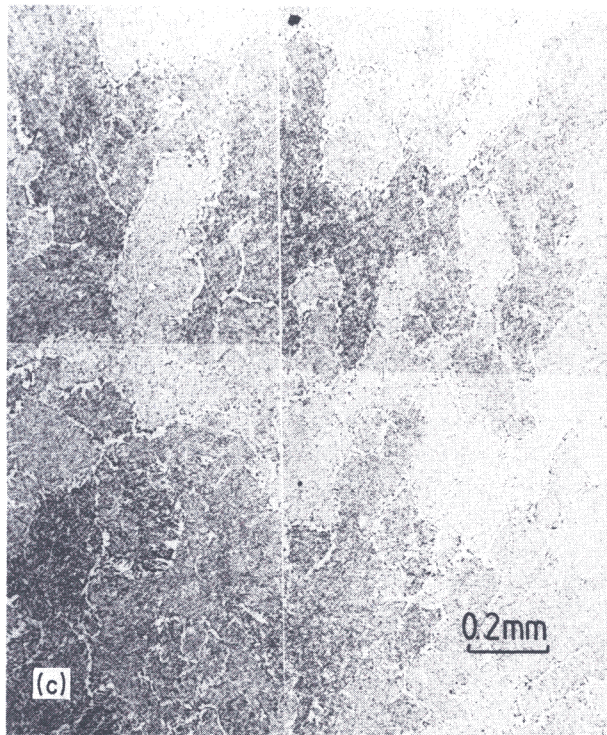
obtained by sectioning parallel to the basal planes of the hexagonal prisms. For this section, from the number of hexagons per unit area, we get

$$\bar{A}_1 = 3a^2 \cos (30°) \qquad (3)$$

Since each hexagon shares a side with its neighbour, the perimeter per hexagon is $3a$, so that the perimeter per unit area of section, $L_A = [a \cos (30°)]^{-1}$. It is a well established stereological rule [20] that $L_A = \pi/2l$ (where $\bar{l}$ is the mean lineal intercept for the section concerned), so that for the longitudinal section,

$$\bar{L}_1 = \pi a \cos (30°)/2 \qquad (4)$$

Values of "a" calculated using Equations 1 to 4 and four different sets of experimental measurements are presented in Table III. For Weld 1 $a = 57$ to $59\,\mu$m and for Weld 2, $a = 45$ to $57\,\mu$m; the reason for the greater dependence of "a" on method and experimental data, in the case of Weld 2, is that the γ grains in this weld deviate from the idealized hexagonal prism shape. The ratio $(\bar{A}/3\overline{aL})$ should equal unity if the grain shape is that of a hexagonal prism with $c \gg a$; Table III shows that this condition is accurately satisfied for Weld 1 but not for Weld 2.

The assumption that $c \gg a$ is justified for the present work: nucleation only occurs at the fusion boundary so that the columnar grains extend all the way to the weld centre line. From the weld geometry, this should give $c \cong 5\,$mm. It can be deduced from Equations 1 and 2 that

$$c = [2.5981a^2 - 3(\bar{A}/\bar{L})\,a]/[(\bar{A}/\bar{L}) - 3a] \qquad (5)$$

"c" calculated for Weld 1 using Equation 5 was found to be about $5\,$mm (Table III) as expected, but could not be determined for Weld 2 for which $\bar{A}/\bar{L} > 3a$
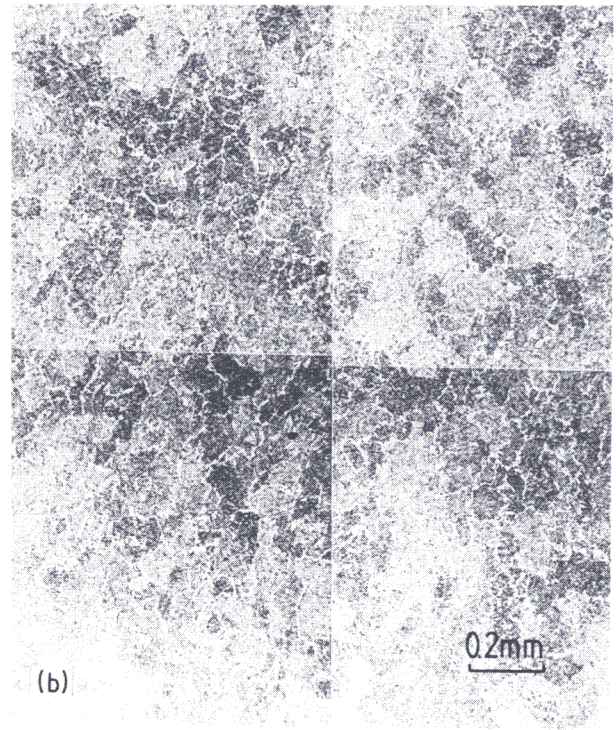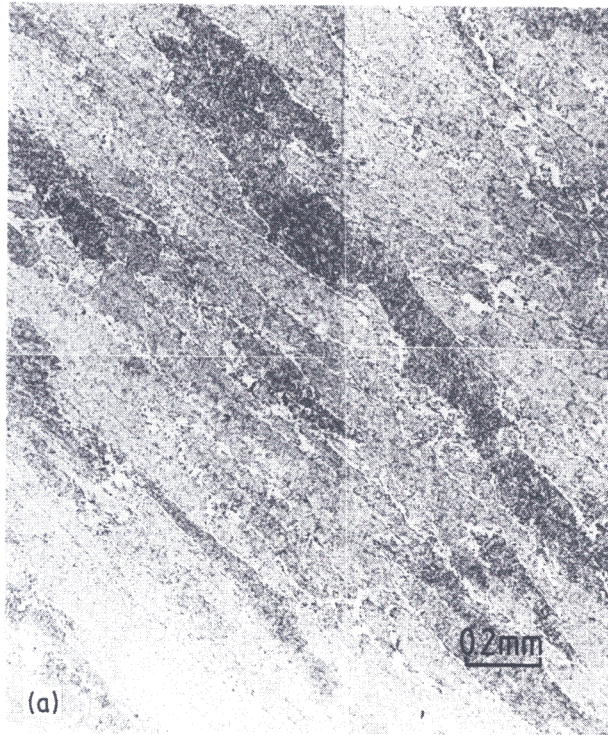
Figure 3 (a) Transverse, (b) longitudinal and (c) inclined sections from the top layer of Weld 2.

since the grains in this case deviate from the hexagonal shape.

The austenite grain size of weld metals has conventionally been represented by a mean lineal intercept determined by superimposing test lines on transverse sections, not in a random orientation relative to the microstructure, but in a direction normal to the major axes of the grain sections. This method has not been formally justified, and it is necessary to deduce how such a measurement (henceforth called $\bar{L}_{tn}$) is related to the parameter "a". If it is assumed that transverse sections represent sections whose normals are parallel or approximately parallel to the basal planes of the

hexagonal prisms, then $\bar{L}_{tn} = \bar{L}_l$. Values of $\bar{L}_{tn}$ presented in Table II are in approximate agreement (within 10%) with corresponding values of $\bar{L}_l$, so that the above assumption seems justified and "a" can be calculated from L_{tn} using Equation 4.

The results discussed above indicate detailed variations in the austenite grain shape, the reasons for which are not understood. The hexagonal prism shape is a good representation of the γ grains of Weld 1 but is less adequate for the γ grains of Weld 2. Nevertheless, the γ grain surface per unit volume, S_V, is similar for the two welds (Table III), so that the hexagonal prism representation can be regarded as adequate for the purpose of microstructure modelling.

From the results presented in Tables II and III an increase in the oxygen content does not lead to a decrease in grain size. Instead, all the measurements indicate that the lower oxygen Weld 2 actually has a slightly smaller γ grain size. These observations are consistent with previous work [9] and indicate that inclusion pinning is not effective at the temperatures where γ grains form from δ ferrite. The anisotropic γ grain morphology is consistent with this since pinning is not expected to be strongly orientation dependent.

Harrison and Farrar [11] reported experiments in which welds with different oxygen concentrations were reheated into the γ phase field, and held there to allow grain coarsening. The resulting equiaxed γ grains were found to decrease in size with increasing oxygen content. This is not inconsistent with the present work because their experiments deal with *reheated* weld metal, the γ grain size being controlled by a coarsening reaction driven by the γ/γ surface energy per unit volume, a driving force amounting to only a few J mol^{-1}. The driving force for the formation

TABLE II Mean lineal and mean areal intercept measurements (in units of μm and μm^2, respectively). N represents the number of intercepts in any experiment, σ is the standard deviation and SE is the standard error as discussed in the text. SE values for $\bar{L}$ and $\bar{A}$ are calculated from the means of the SE values for the three different sections studied

	Weld 1				Weld 2			
	Measurement	σ	N	SE	Measurement	σ	N	SE
$\bar{L}$	100			1.2	86			1.1
$\bar{L}_l$	78	43	3492	0.7	63	37	2100	0.8
$\bar{L}_i$	89	60	3123	1.1	107	79	2435	1.6
$\bar{L}_t$	133	97	3438	1.7	87	55	4924	0.8
$\bar{L}_{tn}$	75	34	2045	0.8	70	37	1621	0.9
$\bar{A}$	16994			2474	17066			2317
$\bar{A}_l$	9053	6829	220	460	5364	4929	188	360
$\bar{A}_i$	11926	10517	168	811	21363	27349	104	2682
$\bar{A}_t$	30004	37402	31	6150	24472	34973	80	3910

of γ from δ-ferrite on the other hand is relatively large, and increases indefinitely with undercooling below the equilibrium transformation temperature; pinning by inclusions cannnot be effective under such circumstances.

Finally, it should be noted that even if the columnar γ grains form directly from the melt by cellular solidification, the cell size at the solid–liquid interface is determined by interface stability [10] in the concentration field ahead of the interface. Oxide and other inclusions which are present in the *liquid* become passively included in the solid by being trapped by the advancing interface, and play no role in influencing the cell size.

4. Conclusions

The columnar austenite grain structure of low-alloy steel, submerged-arc weld deposits can be approximately represented as a honeycomb of hexagonal prisms with $c \gg a$. The "a" parameter can be measured in a number of ways; measurement of then mean lineal intercept in a direction normal to the major axes of grain sections arising in transverse sections of weld deposits gives a reasonable estimate of the parameter "a".

Consistent with earlier work [9], it is found that the oxygen content (121 to 418 p.p.m. by weight) does not determine the size of austenite grains in the as-deposited microstructure. This is probably because the driving force for austenite formation from δ-ferrite is large compared with the force needed to pin the boundaries.

Some detailed variations in austenite grain shape have also been noticed, but the reasons for this are not clear, and need further investigation.

References
1. G. J. DAVIES and J. G. GARLAND, *Int. Metall. Rev.* **20** (1975) 83.
2. W. F. SAVAGE, C. D. LUNDIN and A. H. AARONSON, *Weld J.* **44** (1965) 175.
3. W. F. SAVAGE and A. H. AARONSON, *ibid.* **45** (1966) 85.
4. F. A. CALVO, K. P. BENTLY and R. G. BAKER, "Studies of the Welding Metallurgy of Steels" (BWRA, Abington, Cambridge, 1963) p. 71.
5. D. J. WIDGERY and G. G. SAUNDERS, *Weld. Inst. Res. Bull.* **16** (1975) 277.
6. T. EDVARDSON, H. FREDRIKSSON and I. SVENSSON, *Met. Sci.* **10** (1976) 298.
7. H. FREDRIKSSON and J. STEJERNDAHL, *ibid.* **16** (1982) 575.
8. H. FREDRIKSSON, Acta Universitats Ouluensis, Series C, **26-4**, Proceedings of the 3rd Scandinasm Symposium on Materials Science, 1983 (Oulu University Press, Finland, 1983) p. 1.
9. H. K. D. H. BHADESHIA, L.-E. SVENSSON and B. GRETOFT, *Acta Metall.* **33** (1985) 1271.
10. D. P. WOODRUFF, in "The Solid-Liquid Interface" (Cambridge University Press, Cambridge, 1973) p. 84.
11. P. L. HARRISON and R. A. FARRAR, *J. Mater. Sci.* **16** (1981) 2218.
12. M. FERRANTE and R. A. FARRAR, *ibid.* **17** (1982) 3293.
13. R. C. COCHRANE and P. R. KIRKWOOD, in "Trends in Steels and Consumables for Welding", Proceedings of the Welding Institute Conference, London (1978) p. 103.
14. G. S. BARRITE, R. A. RICKS and P. R. HOWELL, in "Quantitative Microanalysis with High Spatial Resolution", (Metals Society, London, 1981) p. 112.
15. D. J. WIDGERY, Welding Institute Research Members Seminar on the Toughness of Weld Metals, Newcastle-upon-Tyne (1977).
16. F. MATSUDA, *Trans. Nat. Res. Inst. Met. (Jpn.)* **11** (1969) 43.
17. M. KATO, *Trans. Jpn. Weld Soc.* **3** (1972) 69.
18. E. E. UNDERWOOD, "Quantitative Stereology" (Addison-Wesley, Reading Massachusetts, 1970) p. 92.
19. R. T. DEHOFF, "Quantitative Microscopy", edited by R. T. DeHoff and F. N. Rhines, (McGraw-Hill, New York, 1968) p. 12.
20. E. E. UNDERWOOD, in "Quantitative Microscopy", edited by R. T. DeHoff and F. N. Rhines (McGraw-Hill, New York, 1968) p. 78.

TABLE III Results of stereological calculations using the experimental data of Table II. All dimensions have units of μm

	Weld 1	Weld 2
a, calculated using Equation 1b and $\bar{L}$	58	50
a, calculated using Equation 2b and $\bar{A}$	57	57
a, calculated using Equation 3 and $\bar{A}_l$	59	45
a, calculated using Equation 4 and $\bar{L}_l$	57	46
$\bar{a}$ (mean of above "a" values)	58	50
$\bar{A}/(3\bar{a}\bar{L})$ (an index of hexagonality)	0.977	1.323
c, calculated using $\bar{a}$ and Equation 5	5130	
$S_v = 2/\bar{L}$ (μm^{-1})	0.0200	0.0233